

NavigateDiff: Visual Predictors are Zero-Shot Navigation Assistants

Yiran Qin^{1,2*}, Ao Sun^{2*}, Yuze Hong², Benyou Wang², Ruimao Zhang^{1†}

¹ Sun Yat-sen University ² The Chinese University of Hong Kong, Shenzhen
 yiranqin@link.cuhk.edu.cn aosun3@link.cuhk.edu.cn ruimao.zhang@ieee.org

Abstract—Navigating unfamiliar environments presents significant challenges for household robots, requiring the ability to recognize and reason about novel decoration and layout. Existing reinforcement learning methods cannot be directly transferred to new environments, as they typically rely on extensive mapping and exploration, leading to time-consuming and inefficient. To address these challenges, we try to transfer the logical knowledge and the generalization ability of pre-trained foundation models to zero-shot navigation. By integrating a large vision-language model with a diffusion network, our approach named *NavigateDiff* constructs a visual predictor that continuously predicts the agent’s potential observations in the next step which can assist robots generate robust actions. Furthermore, to adapt the temporal property of navigation, we introduce temporal historical information to ensure that the predicted image is aligned with the navigation scene. We then carefully designed an information fusion framework that embeds the predicted future frames as guidance into goal-reaching policy to solve downstream image navigation tasks. This approach enhances navigation control and generalization across both simulated and real-world environments. Through extensive experimentation, we demonstrate the robustness and versatility of our method, showcasing its potential to improve the efficiency and effectiveness of robotic navigation in diverse settings. Project Page: <https://21styouth.github.io/NavigateDiff/>.

I. INTRODUCTION

A useful generalist navigation robot must be able to, much like a human, recognize and reason about novel environments and pathways it has never encountered before. For example, if a user instructs the robot to “find and navigate to that red building,” the robot should be able to accomplish this task even if it has never navigated in that environment or even seen a red building before. In other words, the robot needs not only the physical capability to move through complex environments but also the ability to understand the underlying world rules and perform logical reasoning in environments beyond its training distribution. Although the size of datasets used for robotic navigation has increased in recent years, these datasets cannot possibly cover every environment and scenario the robot might encounter—just as a person’s life experiences cannot include physical interactions with every type of environment. While these datasets provide numerous examples of navigation scenarios, they lack the broad logical knowledge required for robots to navigate the specific environments they may encounter in everyday tasks.

* Equal Contribution; † Corresponding Author

The work is partially supported by Shenzhen Science and Technology Program JCYJ20220818103001002, the Guang.dong Key Laboratory of Big Data Analysis and Processing, Sun Yat-sen University, China, and by the High-performance Computing Public Platform (Shenzhen Campus) of Sun Yat-sen University.

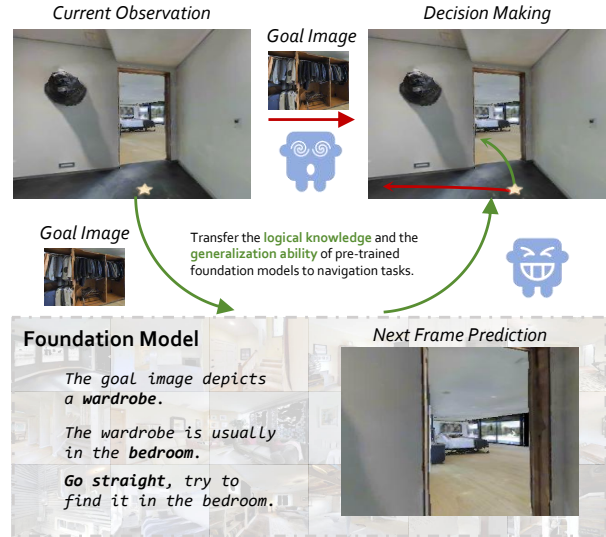


Fig. 1. *NavigateDiff* leverages logical reasoning and generalization capabilities of pre-trained foundation models to enhance zero-shot navigation by predicting future observations to assist robot generate robust actions

Given this, one question naturally arises: how can we integrate this logical knowledge into navigation control? Recently, machine learning methods have achieved broad success in natural language processing [30], visual perception [31], [40], [39], [58], [59], and other domains [32], [33], [44], [42] by leveraging Internet-scale data to train general-purpose “foundation” models. These models are equipped with extensive logical knowledge and can adapt to new tasks through zero-shot transfer, prompt tuning, or fine-tuning on target data [24], [34], [41]. Building on these advancements, researchers in the navigation field have begun to utilize pre-trained foundation models in vision and language to build navigation systems [35] or use pre-trained vision-language encoders to initialize navigation policies [55], [56]. Although these methods aim to incorporate the logical knowledge in Internet-scale data into navigation model training, they (1) often fail to fully exploit the diversity of Internet data, instead being confined to navigation-specific data; (2) merely improve high-level text instruction generalization, which is difficult to apply to specific navigation tasks as the policy network cannot grasp abstract textual concepts.

To address this, we propose *NavigateDiff*, a novel navigation framework to realize generalizable navigation, which introduces the visual predictors to bridge the gap between the high-level trajectory planning in the scene and low-

level policy generation for the robot control. As illustrated in Fig. 1, unlike existing approaches that directly generate robotic policies using current observations and goal images, the proposed method leverages the logical knowledge of foundation models to infer the robot’s next state and generate the corresponding visual content. The results of this visual prediction, along with the original goal image, are then used to assist the policy network in generating specific actions for the robot. In practice, We first construct a **Predictor** by leveraging a large vision-language model followed by a diffusion model. This predictor reasons about the next predicted frame, which is helpful for navigation task execution, by leveraging the goal image, current observation, and optional additional information (such as text instructions or historical observation data). Next, to achieve robot control, we also train a **Hybrid Fusion Policy Network**, which outputs the final control signal by integrating multiple visual information sources, *i.e.* the goal image, current observation, and generated future frame.

Our proposed method has achieved impressive navigation results in both simulation and real-world scenarios. These results are attributed to the fact that our framework decouples the complex high-level reasoning and efficient low-level control required for navigation in open environments. Specifically, when the model needs to analyze and reason about navigation tasks, it can directly leverage the logical knowledge of the vision-language model for effective reasoning, bypassing the need to understand the low-level dynamics of the robot. Conversely, when the model is required to control the robot, the policy network can focus solely on the relationship between the current state and the immediate next state (*i.e.* generated future frame), without the burden of considering long-term task logic or intricate environmental rules. In summary, the main contributions are as follows:

- We propose *NavigateDiff*, a novel navigation framework designed to separate high-level task reasoning from low-level robot control. This decoupling enhances the effectiveness and generalizability of visual navigation.
- We introduce a Predictor that harnesses the advanced reasoning capabilities of large vision-language models to produce a plausible intermediate frame, facilitating downstream robotic control. Additionally, the Hybrid Fusion Policy Network ensures that the generated actions are more stable in practice.
- We conduct extensive experiments in both simulated and real-world settings, yielding numerous experimental results that validate the effectiveness and robustness of our proposed framework.

II. RELATED WORK

A. Vision-based Navigation

Classical SLAM-based methods [1] and learning-based approaches [2], [3], [43], [38] have both been applied to embodied visual navigation. While end-to-end learning techniques tend to rely less on manually designed components, they have demonstrated greater potential. For instance, Memory-Augmented RL [3] employs an attention mechanism that uses

episodic memory to facilitate navigation, achieving state-of-the-art results in ImageNav [50] with four RGB cameras. In contrast, our model adopts a more straightforward architecture and still achieves superior performance. For single-camera setups, [4] enhances performance by incorporating both goal-view rewards and goal-view sampling. We observe that applying this reward system and view sampling leads to further gains for OVRL models.

Similarly, end-to-end reinforcement learning methods have been applied to ObjectNav, utilizing data augmentation [2] and auxiliary rewards [5] to enhance generalization. On the other hand, modular methods [6], [7] separate the tasks of navigation and semantic mapping. A recent competitive imitation learning approach [8], built on a large-scale dataset, offers another direction, which our work builds upon. In contrast to [9], which focuses on improving visual representations by incorporating semantic segmentation, we prioritize RGB-based representations in our approach.

B. Diffusion Models for Image Generation

Recent advances in text-to-image diffusion models [10], [11], [12] have greatly improved instruction-driven image-to-image methods [13], [14], [15], [16] like Instruct-Pix2Pix [13], primarily used for image editing that aims to alter content while keeping the background constant. The method struggles with egocentric images in dynamic, navigation tasks, where the backgrounds change significantly and the images should conform more to physical rules. In this work, we train the MLLM-enhanced diffusion model to generate continuous future images for guiding real-time, low-level control for image navigation tasks.

C. Pretrained Foundation Models for Embodied Tasks

Foundation models like Large Language Models (LLMs) and Diffusion Models have become a powerful tool for prior-knowledge reasoning in navigation, due to their information processing and generative abilities. For example, LLMs are used to predict correlations with the target object at both the object and room levels, aiding in locating the target [17], [19]. They also help cluster unexplored areas and infer relationships between the target and surrounding objects to guide navigation [18], [21]. Chain-of-thought (CoT) reasoning is integrated into LLMs to encourage exploration in areas likely to contain the target while avoiding irrelevant regions [20]. In multi-robot collaborative navigation, LLMs centrally plan mid-term goals by analyzing data such as obstacles, frontiers, and object coordinates from online maps [22]. Furthermore, path and farsight descriptions are combined to enable LLMs to apply commonsense reasoning for waypoint identification [23]. Additionally, Diffusion Models have made significant advances in embodied scenarios. For instance, video diffusion is combined with inverse dynamics to generate robot control signals for specific tasks [25], [26]. In another approach, diffusion models are used for interpretable hierarchical planning through skill abstractions during task execution [27]. Furthermore, these models are employed to guide agents through open-ended tasks [24], [16].

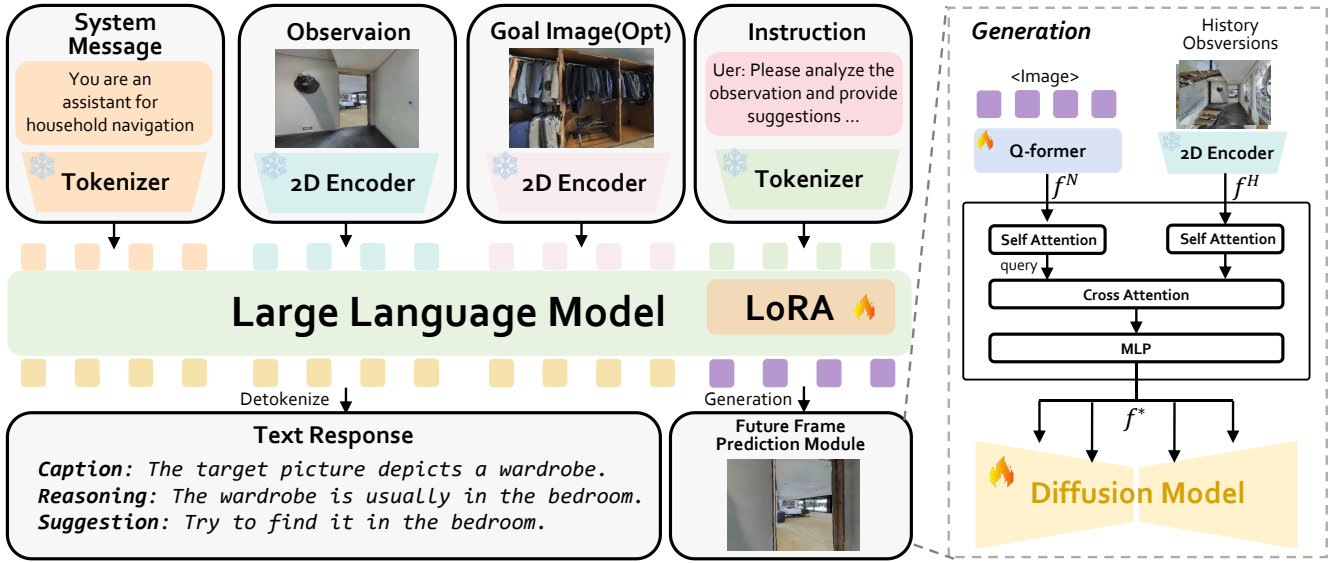


Fig. 2. **The Overall Architecture of Predictor.** Instruction, current observation, and goal image are encoded separately and sent into LLaVA [36]. Then LLaVA [36] generates hidden states for the Special Image Tokens $\langle \text{image} \rangle$ tokens, we transform $\langle \text{image} \rangle$ into semantically relevant representations f^N using a Q-Former. The feature f^H , extracted from the 2D encoder, is fused with the feature f^N . The resulting fused feature f^* is then used as a condition in the Edit-based diffusion model to generate future images.

III. METHOD

NavigateDiff utilizes the logical knowledge and the generalization ability of pre-trained foundation models to improve zero-shot navigation in the presence of novel environments, scenes, and objects. How can we achieve this when foundation models trained on general-purpose Internet data do not provide direct guidance for selecting low-level navigation actions? Our key insight is to decouple the navigation problem into two stages: (I) generating intermediate future goals that need to be reached to successfully navigate, and (II) learning low-level control policies for reaching these future goals. In Stage (I), we build a **Predictor** by incorporating a Multimodal Large Language Model (MLLM) with a diffusion model, fine-tuned with parameter efficiency, specifically designed for Image Navigation [50]. Stage (II) involves training a **Fusion Navigation Policy** on image navigation data and testing in new environments. We describe data collection and each of these stages in detail below and summarize the resulting navigation algorithm.

A. Data Formulation

For the generation of future frame training data, we utilized the simulator’s built-in “shortest path follower” algorithm in the simulation environment to obtain the standard route for each task and generate corresponding videos. In the real world, we recorded ego-view perspective videos of a human remotely controlling a navigation robot to complete the image navigation tasks. Based on the collected videos, we randomly selected a starting frame from each video and chose the corresponding future frame according to a pre-defined prediction interval k . We also recorded the relevant navigation task information, ultimately forming the training tuples $(x_t, x_{t+k}, x_h, y, x_g)$. where x_t represents the current

observation image, x_{t+k} is the future frame image that needs to be predicted, x_h is the history frame of x_t , y indicates the task’s corresponding textual instruction and x_g is the final goal image for the navigation task.

B. Predictor

As illustrated in Fig. 2, our Predictor integrates a **Multi-modal Large Language Model (MLLM)** with a **Future Frame Prediction Model**, which could process current observations, target images, and instructions and generate a predicted future image based on the provided input.

Multimodal Large Language Model. Given a current observation x_t , a goal image x_g , and a textual instruction y , the Predictor generates a future frame. As shown in Fig. 2, the current observation and goal image are processed through a frozen image encoder, while the textual instruction is tokenized and passed to the LLM. The Predictor can now generate Special Image Tokens $\langle \text{image} \rangle$ based on the instruction’s intent, though initially limited to the language modality. These tokens are then sent to the Future Frame Prediction Model to produce the final future frame prediction. In practice, we utilized LLaVA as our base model, which consists of a pre-trained CLIP visual encoder (ViT-L/14) and Vicuna-7B as the LLM backbone. To fine-tune the LLM, we applied LoRA, initializing a trainable matrix to adapt the model for the task.

Future Frame Prediction Model. For future frame generation, we bridge the gap between the LLM’s hidden states and the LLaVA text encoder’s spaces, we transform the Special Image Tokens $\langle \text{image} \rangle$ into semantically relevant representations f^N using a Q-Former. The feature f^H , extracted from the 2D encoder, is fused with the feature f^N . The resulting fused feature f^* is then used as a condition

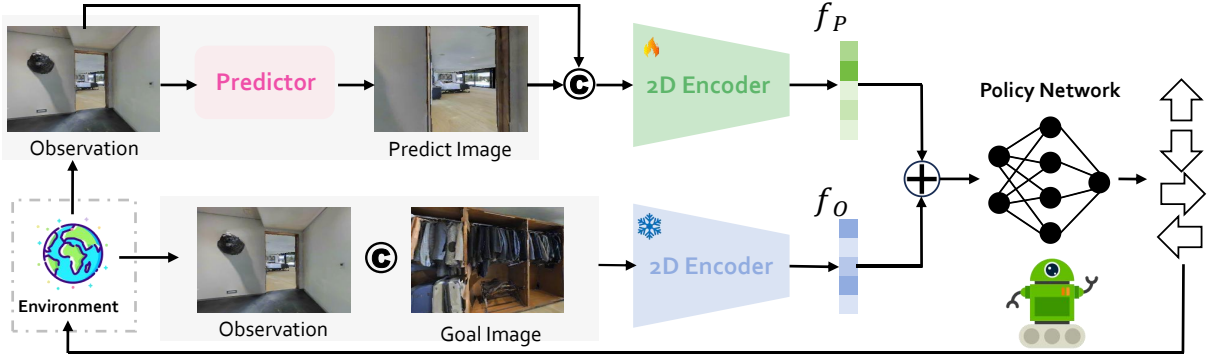


Fig. 3. *NavigateDiff* leverages a Future Frame pretrained Predictor to generate future frames based on current observation and navigation task information. A fusion navigation policy then executes the actions needed to reach the future frames. Alternating this loop enables us to accomplish the navigation task.

in the Edits-based diffusion model [51] to generate future images:

$$f^* = \mathbf{H}(\mathbf{Q}(h_{\langle image \rangle}), \mathbf{E}_v(x_h)) \quad (1)$$

where \mathbf{Q} denotes the Q-Former, \mathbf{E}_v is a 2D encoder, $\mathbf{E}_v(x_h)$ indicates history observations, and \mathbf{H} is the fusion block that includes two self-attention blocks, a cross-attention block, and an MLP layer.

We employ a latent diffusion model with a VAE to perform denoising diffusion in the latent space, conditioned on fused feature f^* . Formally, the training objective is given by:

$$\mathcal{L}_{\text{predictor}} = \mathbb{E}_{\mathcal{E}(x_{t+k}), \mathcal{E}(x_t), \epsilon \sim \mathcal{N}(0,1), s} [\|\epsilon - \epsilon_{\delta}(s, [z_s, \mathcal{E}(x_t)] + f^*)\|_2^2] \quad (2)$$

where ϵ represents unscaled noise, s denotes the sampling step, and z_s is the latent noise at step s . The term $\mathcal{E}(x_t)$ corresponds to the current observation condition.

By incorporating temporal information, this hybrid approach captures object trajectories and richer scene semantics, allowing for more accurate predictions of object movements and environmental changes. This makes our method particularly effective for zero-shot navigation in dynamic scenes. Dataset construction and implementation details can be found in IV-A.

C. Fusion Navigation Policy

Although the Predictor provides one-step future state planning within the vision modality, we also need to train a low-level controller to select appropriate navigation actions. As the Predictor generates future frame images infused with prior knowledge from the pre-trained foundation model, our approach requires only the design of an image fusion navigation policy to effectively leverage the foundational model’s logical reasoning and generalization capabilities for robot navigation tasks.

Image Fusion Policy. During the training phase, the current observation x_t is concatenated with the future frame x_{t+k} along the RGB channel dimension and processed through a trainable 2D Encoder to obtain f_p . The current observation x_t is also concatenated with the final goal image x_g along the RGB channel dimension and passed through a pre-trained 2D Encoder to obtain f_o . Based on the fused

representations of the future and goal images, we train a navigation policy π using reinforcement learning (RL):

$$s_t = \pi([f_p, f_o, a_{t-1}] | h_{t-1}) \quad (2)$$

where s_t represents the embedding of the agent’s current state, and h_{t-1} denotes the hidden state of the recurrent layers in the policy π from the previous step. We employ an actor-critic network [4] to predict both the state value and the action a_t using s_t , training the model end-to-end with PPO [53].

During the testing phase, we utilize trained Predictor and Fusion Navigation Policy to navigate in new environments based on corresponding goal images. For the image navigation task with a goal image x_g , given a current observation x_t , we generate the next future frame $x_t^* \leftarrow \mathcal{G}(x_t, x_g, y)$, once the future frame is sampled, we then execute the Fusion Navigation Policy π conditioned on x_t^*, x_t, x_g for k timesteps, where k is a testing hyperparameter. After k timesteps, the future frame is refreshed by sampling from the Predictor again, and the process is repeated. Conventional wisdom suggests that regenerating future frames more frequently could result in more robust navigation control, assuming an unlimited computational budget. However, in practice, to maintain computational efficiency, we set k to closely match the corresponding timesteps used during training, which has consistently delivered satisfactory performance. The pseudocode for navigation testing is detailed in Algorithm. 1.

Algorithm 1 NavigateDiff: Zero-Shot Navigation Testing

Require: Predictor \mathcal{G} , Fusion Policy π , time limit T , future frame generation interval k , goal image x_g , instruction y

- 1: $t \leftarrow 0$
- 2: **while** $t < T$ **do**
- 3: $x_t^* \leftarrow \mathcal{G}(x_t, x_g, y)$
- 4: **for** $i = 1$ to k **do**
- 5: $a_t \leftarrow \pi(x_t^*, x_t, x_g)$
- 6: Execute a_t
- 7: $x_{t+1} \leftarrow \text{Environment}$
- 8: $t \leftarrow t + 1$
- 9: **end for**
- 10: **end while**

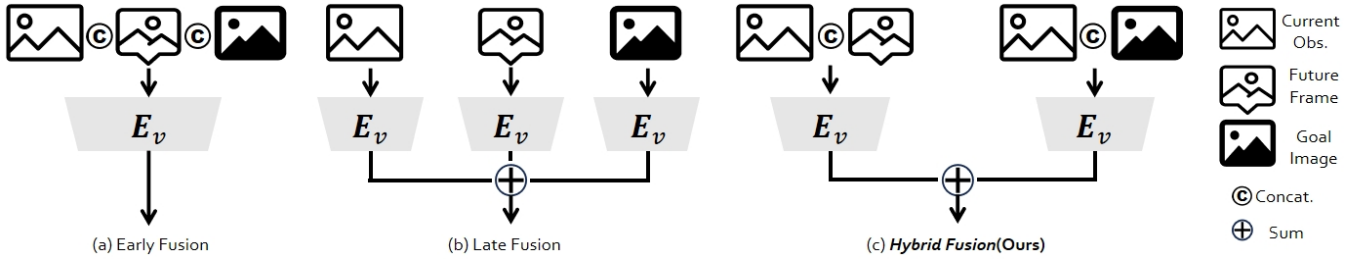


Fig. 4. Comparison of different image fusion strategies (a) Early Fusion, (b) Late Fusion, and (c) **Hybrid Fusion(Ours)**.

TABLE I

QUANTITATIVE COMPARISON (FID↓, PSNR↑, LPIPS↓). IP2P HAS ALSO BEEN FINE-TUNED USING THE NAVIGATION TRAINING DATA.

Setting	FID↓	PSNR↑	LPIPS↓
IP2P[13]	26.59	14.59	42.25
Predictor(Ours)	25.93	14.73	40.82



Fig. 5. Example rollouts in Gibson dataset.

Fusion Strategy Design. As shown in Fig. 4, we designed a Hybrid Fusion approach to fuse image features and compared its performance with Early Fusion and Late Fusion. In Early Fusion, the current observation, future frame prediction, and goal image are concatenated along the RGB channels and then passed through a visual encoder for feature extraction. While this method can capture pixel-level semantic relationships among the three images, it struggles to effectively associate the logical relationships among them. In contrast, Late Fusion processes the three images separately through the visual encoder and then fuses them at the feature level, but this approach fails to capture pixel-level semantic correlations, leading to suboptimal performance.

Our proposed Hybrid Fusion takes a different approach: one branch concatenates the current observation and future frame prediction along the RGB channels, while another branch concatenates the current observation and goal image. This not only establishes semantic associations at the pixel level but also separates local information (from the current observation to the future frame prediction) and global information (from the current observation to the goal image) in the temporal dimension, resulting in superior performance.

IV. EXPERIMENTS

A. Predictor

Dataset. We used the dataset format constructed in Sec. III-A and collected video sequences from all image navigation

TABLE II

COMPARISON WITH STATE-OF-THE-ART METHODS ON GIBSON.

Method	Train Dataset	Sensor(s)	SPL	SR
NTS [1]	Full	RGBD+Pose	43.0%	63.0%
Act-Neur-SLAM [1]	Full	RGB+Pose	23.0%	35.0%
SPTM [45]	Full	RGB+Pose	27.0%	51.0%
ZER [4]	Full	RGB	21.6%	29.2%
ZSON [46]	Full	RGB	28.0%	36.9%
OVRL [47]	Full	RGB	27.0%	54.2%
OVRL-V2 [48]	Full	RGB	58.7%	82.0%
FGPrompt	Full	RGB	66.5%	90.4%
NavigateDiff(Ours)	Full	RGB	64.8%	91.0%
FGPrompt [49]	1/4	RGB	48.5%	77.9%
NavigateDiff(Ours)	1/4	RGB	52.1%	81.2%
FGPrompt [49]	1/8	RGB	43.4%	68.1%
NavigateDiff(Ours)	1/8	RGB	46.4%	71.1%

tasks in the GIBSON dataset’s training set for training. The interval hyperparameter was set to $k = 5$ during the training process.

Training Process. The training process of the Predictor consists of two key stages. First, InstructPix2Pix [13] is used to pre-train the diffusion model weights in the navigation environment. Next, the Predictor is optimized in an end-to-end fashion. The diffusion model’s initial weights in the Predictor are taken directly from those pre-trained in the first stage.

Evaluation. We implement three image-level metrics to evaluate the Predictor’s generation ability. (1) Fréchet Inception Distance (FID) [28], (2) Peak Signal-to-Noise Ratio (PSNR), (3) Learned Perceptual Image Patch Similarity (LPIPS) [29]. We measure the similarity between the generated future frame and ground truth. In terms of image-level metrics in Tab. I, our Predictor outperforms IP2P by a large margin (0.66, 0.14, and 1.43 respectively) in all three metrics on the Gibson dataset. In Fig. 5, we also visualize predicted future frame sequences and trajectory rollouts in the Gibson dataset. We observe that generating future frames one by one could efficiently guide the PolicyNet in action generation.

B. Simulation Experiments

Dataset For image-goal navigation, we employ the Habitat simulator and train our agent on the Gibson dataset, using 72 training scenes and 14 testing scenes under the standard configuration. We train the agent for 500M steps, following the rules as outlined in FGPrompt [49]. Results are reported across multiple datasets to enable direct comparison with

TABLE III
CROSS-DOMAIN EVALUATION ON MP3D. THE AGENT IS TRAINED IN GIBSON ENVIRONMENTS AND DIRECTLY TRANSFERRED TO NEW ENVIRONMENTS FOR EVALUATION.

Methods	Train Dataset	SPL	SR
Mem-Aug [3]	Gibson	3.9%	6.9%
NRNS [57]	Gibson	5.2%	9.3%
ZER [4]	Gibson	10.8%	14.6%
FGPrompt [49]	1/4 Gibson	37.1%	65.7%
NavigateDiff (Ours)	1/4 Gibson	41.1%	68.0%
FGPrompt [49]	1/8 Gibson	31.8%	55.0%
NavigateDiff (Ours)	1/8 Gibson	34.9%	57.7%

TABLE IV
COMPARING IN THREE DIVERSE REAL-WORLD ENVIRONMENTS SCENES. (OFFICE, PARKING LOT AND CORRIDOR).

Methods	Office		Parking Lot		Corridor	
	SPL	SR	SPL	SR	SPL	SR
FGPrompt [49]	41.0%	50.0%	52.3%	64.3%	54.8%	71.4%
NavigateDiff (Ours)	41.2%	57.1%	51.1%	71.4%	55.6%	78.6%

previous works. For the Gibson dataset, we validate our agent on split A generated by [3]. For the MP3D datasets, we use test episodes collected by [4] and the instance image navigation dataset released by [52].

Setting We report the Success Rate (SR) and Success weighted by Path Length (SPL) [54], which accounts for the efficiency of the navigation path. An episode is deemed successful if the agent stops within a 1.0m Euclidean distance from the goal. The maximum number of steps per episode is set to 500 by default. In agent configuration, We follow the setup outlined in prior works [4] [46] [47] [49] to initialize an agent equipped with RGB cameras, featuring a 128×128 resolution and a 90° field of view (FOV). The agent’s action space includes four discrete actions—MOVE_FORWARD, TURN_LEFT, TURN_RIGHT, and STOP—with minimum rotation and forward movement units set to 30° and 0.25m, respectively.

Result In Tab. II, we present a detailed comparison between our model and several state-of-the-art approaches across various metrics. The results highlight the superior performance of our model, particularly in challenging navigation scenarios. To further evaluate the generalization capability of our approach, we conducted additional experiments using a smaller dataset that poses a greater challenge in terms of data availability. Despite the reduced dataset size, our model not only maintained its performance but also outperformed the baseline models. This demonstrates the robustness and adaptability of our model, suggesting it can effectively generalize to new environments even with limited training data.

As illustrated in Tab. III, we test the model on the MP3D dataset as part of a cross-task evaluation. Our *NavigateDiff* achieves 68.0% Success Rate (SR) and 41.1% Success weighted by Path Length (SPL) by using a smaller training dataset, surpassing both existing methods on the full dataset and the baseline.



Fig. 6. Scenes in Real-world Environment, from the left, in the order of Corridor, Office and Parking Lot

TABLE V
DIFFERENT FUSION STRATEGIES ON GIBSON IMAGENAV TASK.

Setting	SPL	SR
Late Fusion	11.7%	13.7%
Early Fusion	20.5%	40.1%
Hybrid Fusion	64.8%	91.0%

C. Real-world Experiments

Setting In our real-world experiments, we focused on indoor environments to evaluate the zero-shot navigation capabilities of our model, *NavigateDiff*. As illustrated in Fig. 6, we conducted tests in three types of indoor environments: an office, a parking lot, and a corridor. Each environment represents a unique set of challenges in terms of layout, lighting, and obstacles. The office setting is characterized by cluttered spaces, including desks, chairs, and other furniture. The indoor parking lot represents a semi-structured environment with clearly defined paths and open spaces but is filled with parked vehicles that act as static obstacles. The corridor is a long, narrow space with fewer obstacles but presents challenges in terms of navigation through tight spaces and sharp turns.

Result As detailed in Tab. IV, We evaluate the performance of *NavigateDiff* in terms of success rate and SPL. The metric across the three real-world scenarios demonstrates that our model consistently surpasses the baseline.

Overall, *NavigateDiff* demonstrates strong zero-shot navigation capabilities across all environments. The model’s ability to adapt to different layouts and lighting conditions without prior training in those specific environments highlights its robustness in real-world applications.

D. Fusion Strategy Design

As shown in Tab. V, we evaluate different fusion strategies on the Gibson ImageNav task. Our proposed Hybrid Fusion achieves 91.0% SR and 64.8% SPL, significantly outperforming both Early Fusion and Late Fusion. These results demonstrate the effectiveness of Hybrid Fusion in integrating future frames into the navigation policy.

V. CONCLUSIONS

We introduced *NavigateDiff*, a novel approach that leverages logical reasoning and generalization capabilities of pre-trained foundation models to enhance zero-shot navigation by predicting future observations for robust action generation. By integrating temporal information and using a Hybrid Fusion framework to guide policy decisions, our approach significantly improves navigation performance. Extensive experiments demonstrate its efficiency and adaptability in both simulated and real-world environments.

REFERENCES

- [1] Chaplot, Devendra Singh, et al. "Neural topological slam for visual navigation." *Proceedings of the IEEE/CVF conference on computer vision and pattern recognition*. 2020.
- [2] Maksymets, Oleksandr, et al. "Thda: Treasure hunt data augmentation for semantic navigation." *Proceedings of the IEEE/CVF International Conference on Computer Vision*. 2021.
- [3] Mezghan, Lina, et al. "Memory-augmented reinforcement learning for image-goal navigation." *2022 IEEE/RSJ International Conference on Intelligent Robots and Systems (IROS)*. IEEE, 2022.
- [4] Al-Halah, Ziad, Santhosh Kumar Ramakrishnan, and Kristen Grauman. "Zero experience required: Plug & play modular transfer learning for semantic visual navigation." *Proceedings of the IEEE/CVF Conference on Computer Vision and Pattern Recognition*. 2022.
- [5] Ye, Joel, et al. "Auxiliary tasks and exploration enable objectgoal navigation." *Proceedings of the IEEE/CVF international conference on computer vision*. 2021.
- [6] Chaplot, Devendra Singh, et al. "Object goal navigation using goal-oriented semantic exploration." *Advances in Neural Information Processing Systems* 33 (2020)
- [7] Ramakrishnan, Santhosh Kumar, et al. "Poni: Potential functions for objectgoal navigation with interaction-free learning." *Proceedings of the IEEE/CVF Conference on Computer Vision and Pattern Recognition*. 2022.
- [8] Ramrakhya, Ram, et al. "Habitat-web: Learning embodied object-search strategies from human demonstrations at scale." *Proceedings of the IEEE/CVF Conference on Computer Vision and Pattern Recognition*. 2022.
- [9] Mousavian, Arsalan, et al. "Visual representations for semantic target driven navigation." *2019 International Conference on Robotics and Automation (ICRA)*. IEEE, 2019.
- [10] Dhariwal, Prafulla, and Alexander Nichol. "Diffusion models beat gans on image synthesis." *Advances in neural information processing systems* 34 (2021)
- [11] Ho, Jonathan, and Tim Salimans. "Classifier-free diffusion guidance." *arXiv preprint arXiv:2207.12598* (2022).
- [12] Nichol, Alex, et al. "Glide: Towards photorealistic image generation and editing with text-guided diffusion models." *arXiv preprint arXiv:2112.10741* (2021)
- [13] Brooks, Tim, Aleksander Holynski, and Alexei A. Efros. "Instruct-pix2pix: Learning to follow image editing instructions." *Proceedings of the IEEE/CVF Conference on Computer Vision and Pattern Recognition*. 2023.
- [14] Fu, Tsu-Jui, et al. "Guiding instruction-based image editing via multimodal large language models." *arXiv preprint arXiv:2309.17102* (2023).
- [15] Geng, Ziang, et al. "Instructdiffusion: A generalist modeling interface for vision tasks." *Proceedings of the IEEE/CVF Conference on Computer Vision and Pattern Recognition*. 2024.
- [16] Zhou, Enshen, et al. "Minedreamer: Learning to follow instructions via chain-of-imagination for simulated-world control." *arXiv preprint arXiv:2403.12037* (2024).
- [17] Zhou, Kaiwen, et al. "Esc: Exploration with soft commonsense constraints for zero-shot object navigation." *International Conference on Machine Learning*. PMLR, 2023.
- [18] Yu, Bangguo, Hamidreza Kasaei, and Ming Cao. "L3mvm: Leveraging large language models for visual target navigation." *2023 IEEE/RSJ International Conference on Intelligent Robots and Systems (IROS)*. IEEE, 2023.
- [19] Gadre, Samir Yitzhak, et al. "Cows on pasture: Baselines and benchmarks for language-driven zero-shot object navigation." *Proceedings of the IEEE/CVF Conference on Computer Vision and Pattern Recognition*. 2023.
- [20] Shah, Dhruv, et al. "Navigation with large language models: Semantic guesswork as a heuristic for planning." *Conference on Robot Learning*. PMLR, 2023.
- [21] Cai, Wenzhe, et al. "Bridging zero-shot object navigation and foundation models through pixel-guided navigation skill." *2024 IEEE International Conference on Robotics and Automation (ICRA)*. IEEE, 2024.
- [22] Yu, Bangguo, Hamidreza Kasaei, and Ming Cao. "Co-NavGPT: Multi-robot cooperative visual semantic navigation using large language models." *arXiv preprint arXiv:2310.07937* (2023).
- [23] Wu, Pengying, et al. "Voronav: Voronoi-based zero-shot object navigation with large language model." *arXiv preprint arXiv:2401.02695* (2024).
- [24] Qin, Yiran, et al. "Mp5: A multi-modal open-ended embodied system in minecraft via active perception." *arXiv preprint arXiv:2312.07472* (2023).
- [25] Du, Yilun, et al. "Learning universal policies via text-guided video generation." *Advances in Neural Information Processing Systems* 36 (2024).
- [26] Ajay, Anurag, et al. "Compositional foundation models for hierarchical planning." *Advances in Neural Information Processing Systems* 36 (2024).
- [27] Liang, Zhixuan, et al. "Skilldiffuser: Interpretable hierarchical planning via skill abstractions in diffusion-based task execution." *Proceedings of the IEEE/CVF Conference on Computer Vision and Pattern Recognition*. 2024.
- [28] Heusel, Martin, et al. "Gans trained by a two time-scale update rule converge to a local nash equilibrium." *Advances in neural information processing systems* 30 (2017).
- [29] Zhang, Richard, et al. "The unreasonable effectiveness of deep features as a perceptual metric." *Proceedings of the IEEE conference on computer vision and pattern recognition*. 2018.
- [30] Brown, Tom B. "Language models are few-shot learners." *arXiv preprint arXiv:2005.14165* (2020).
- [31] Podell, Dustin, et al. "Sdxl: Improving latent diffusion models for high-resolution image synthesis." *arXiv preprint arXiv:2307.01952* (2023).
- [32] Brohan, Anthony, et al. "Rt-1: Robotics transformer for real-world control at scale." *arXiv preprint arXiv:2212.06817* (2022).
- [33] Brohan, Anthony, et al. "Rt-2: Vision-language-action models transfer web knowledge to robotic control." *arXiv preprint arXiv:2307.15818* (2023).
- [34] Li, Xiaoqi, et al. "Manipllm: Embodied multimodal large language model for object-centric robotic manipulation." *Proceedings of the IEEE/CVF Conference on Computer Vision and Pattern Recognition*. 2024.
- [35] Shah, Dhruv, et al. "ViNT: A foundation model for visual navigation." *arXiv preprint arXiv:2306.14846* (2023).
- [36] Liu, Haotian, et al. "Visual instruction tuning." *Advances in neural information processing systems* 36 (2024).
- [37] Hu, Edward J., et al. "Lora: Low-rank adaptation of large language models." *arXiv preprint arXiv:2106.09685* (2021).
- [38] Qin, Yiran, et al. "SupFusion: Supervised LiDAR-camera fusion for 3D object detection." *Proceedings of the IEEE/CVF International Conference on Computer Vision*. 2023.
- [39] Qin, Yiran, et al. "Worldsimbench: Towards video generation models as world simulators." *arXiv preprint arXiv:2410.18072* (2024).
- [40] Yu, Jiwen, et al. "GameFactory: Creating New Games with Generative Interactive Videos." *arXiv preprint arXiv:2501.08325* (2025).
- [41] Zhou, Enshen, et al. "Code-as-Monitor: Constraint-aware Visual Programming for Reactive and Proactive Robotic Failure Detection." *arXiv preprint arXiv:2412.04455* (2024).
- [42] Zhang, Zaibin, et al. "AD-H: Autonomous Driving with Hierarchical Agents." *arXiv preprint arXiv:2406.03474* (2024).
- [43] Wang, Chaoqun, et al. "Toward Accurate Camera-based 3D Object Detection via Cascade Depth Estimation and Calibration." *arXiv preprint arXiv:2402.04883* (2024).
- [44] Huang, Yuzhou, et al. "Story3d-agent: Exploring 3d storytelling visualization with large language models." *arXiv preprint arXiv:2408.11801* (2024).
- [45] Savinov, Nikolay, Alexey Dosovitskiy, and Vladlen Koltun. "Semi-parametric topological memory for navigation." *arXiv preprint arXiv:1803.00653* (2018).
- [46] Majumdar, Arjun, et al. "Zson: Zero-shot object-goal navigation using multimodal goal embeddings." *Advances in Neural Information Processing Systems* 35 (2022): 32340-32352.
- [47] Yadav, Karmesh, et al. "Offline visual representation learning for embodied navigation." *Workshop on Reincarnating Reinforcement Learning at ICLR*. 2023.
- [48] Yadav, Karmesh, et al. "Ovrl-v2: A simple state-of-art baseline for imagenav and objectnav." *arXiv preprint arXiv:2303.07798* (2023).
- [49] Sun, Xinyu, et al. "FGPrompt: fine-grained goal prompting for image-goal navigation." *Advances in Neural Information Processing Systems* 36 (2024).

- [50] Zhu, Yuke, et al. "Target-driven visual navigation in indoor scenes using deep reinforcement learning." 2017 IEEE international conference on robotics and automation (ICRA). IEEE, 2017.
- [51] Koh, Jing Yu, Daniel Fried, and Russ R. Salakhutdinov. "Generating images with multimodal language models." *Advances in Neural Information Processing Systems* 36 (2024).
- [52] Krantz, Jacob, et al. "Instance-specific image goal navigation: Training embodied agents to find object instances." *arXiv preprint arXiv:2211.15876* (2022).
- [53] Schulman, John, et al. "Proximal policy optimization algorithms." *arXiv preprint arXiv:1707.06347* (2017).
- [54] Anderson, Peter, et al. "On evaluation of embodied navigation agents." *arXiv preprint arXiv:1807.06757* (2018).
- [55] Lin, Bingqian, et al. "NavCoT: Boosting LLM-Based Vision-and-Language Navigation via Learning Disentangled Reasoning." *arXiv preprint arXiv:2403.07376* (2024).
- [56] Zhou, Gengze, Yicong Hong, and Qi Wu. "Navgpt: Explicit reasoning in vision-and-language navigation with large language models." *Proceedings of the AAAI Conference on Artificial Intelligence*.
- [57] Hahn, Meera, et al. "No rl, no simulation: Learning to navigate without navigating." *Advances in Neural Information Processing Systems* 34 (2021): 26661-26673.
- [58] Li, Lijun, et al. "T2ISafety: Benchmark for Assessing Fairness, Toxicity, and Privacy in Image Generation." *arXiv preprint arXiv:2501.12612* (2025).
- [59] An, Jingkun, et al. "AGFSync: Leveraging AI-Generated Feedback for Preference Optimization in Text-to-Image Generation." *arXiv preprint arXiv:2403.13352* (2024).